SEGREGATION EFFECT ON MICROSTRUCTURE STABILITY & MECHANICAL PROPERTIES OF Mg-0.4 wt% Ca ALLOY

M.Tech. Thesis

By

SHUBHAM GARG

DEPARTMENT OF METALLURGY ENGINEERING AND MATERIALS SCIENCE

INDIAN INSTITUTE OF TECHNOLOGY INDORE

June 2022

SEGREGATION EFFECT ON MICROSTRUCTURE STABILITY AND MECHANICAL PROPERTIES OF Mg-0.4 wt% Ca ALLOY

A THESIS

Submitted in partial fulfillment of the
Requirements for the award of the degree

Of
Master of Technology

by

SHUBHAM GARG

DEPARTMENT OF METALLURGY ENGINEERING AND MATERIALS SCIENCE

INDIAN INSTITUTE OF TECHNOLOGY INDORE

June 2022

INDIAN INSTITUTE OF TECHNOLOGY INDORE

CANDIDATE'S DECLARATION

I hereby certify that the work which is being presented in the thesis entitled **SEGREGRATION EFFECT ON MICROSTRUCTURE STABILITY AND MECHANICAL PROPERTIES OF Mg-0.4wt% Ca ALLOY** in the partial fulfillment of the requirements for the award of the degree of **MASTERS OF TECHNOLOGY** in **METALLURGY ENGINEERING** and submitted in the **DEPARTMENT OF METALLURGY ENGINEERING AND MATERIALS SCIENCE,** Indian Institute of Technology Indore, is an authentic record of my work carried out during the time period from July 2021 to May 2022 under the supervision of Dr. Dudekula Althaf Basha, Assistant Professor, Department of Metallurgy Engineering and Materials Science, Indian Institute of Technology, Indore.

I have not submitted the matter presented in this thesis for the award of any other degree of this or any other institute.

Shubham garg
07/06/2022
SHUBHAM GARG

This is to certify that the above statement made by the candidate is correct to the best of my/our knowledge.

D. Althaf Basha
07/06/2022
Dr. Dudekula Althaf Basha

SHUBHAM GARG has successfully given his M.Tech Oral examination held on **02/06/2022.**

D. Althaf Basha
07/06/2022
Dr. Dudekula Althaf Basha

(A.K. Kushwaha)
Dr. A.K. Kushwaha (Acting DPGC Conv.)
13/06/2022
Dr. Sumanta samal
Convener, DPGC

K. Eswara Prasad
8.6.2022
Dr. Eswara Prasad korimilli
Signature of PSPC Member

08/06/2022
Dr. Indrasen singh
Signature of PSPC Member

ACKNOWLEDGMENTS

First and foremost, I am very thankful to my research supervisor Dr. Dudekula Althaf Basha for the continuous support and advices and counseling in my research work. His friendly interactions and constructive support have enabled this work to achieve its present form. Despite being busy with a lot of administrative roles, he never failed to spend enough time on the research activities and discussing academics and research-related things with his students including me. His time management skills always amazed me. His knowledge and the skills to communicate them simply and effectively are great and really helped me to gain a conceptual understanding of many topics needed to carry out my research effectively.

I would like to take this opportunity to thank my PSPC members, Dr. Eswara Prasad K. and Dr. Indrasen Singh for their valuable time in assessing my work and for the valuable suggestions and insightful comments.

I am thankful to Dr. Vinod Kumar, HOD (Dept. of MEMS) for his support and cooperation. I am thankful to all faculty members and staff of the Department of Metallurgy Engineering and Materials Science for their guidance, help and support. I am thankful to MHRD, Govt. of India, for providing fellowship during my Master studies.

Last but not least, I cannot forget the support and encouragement received from my family and my colleges.

Abstract

Despite the large amount of work done in the last two decades on light weight magnesium (Mg) alloys, there is a lack of systematic and careful study on the effect of segregation on microstructure stability of Mg alloys. In previous studies, small precipitates were found at grain boundaries along with segregation in dilute magnesium alloys. Hence, it was not clear whether grain growth was hindered by grain boundary pinning effect or segregation effect. Furthermore, in earlier studies the amount of segregation was not uniform across the boundaries. Hence, the aim of present study is to study the effect of Ca as a segregating element on the microstructure stability of dilute magnesium alloys. In this context, Mg - 0.4wt% Ca alloys were processed by high pressure torsion (HPT) and extrusion techniques. Ca segregation was observed along the grain boundaries in extruded alloys, whereas no segregation was observed in HPT processed alloys. Microstructure stability experiments show that the grain size of the extruded alloys with grain boundary segregation has not increased to a greater extent after heat treatment. Whereas, the grain size of the HPT alloys without grain boundary segregation has increased quite an extent, hence, its microstructure is least stable with respect to heat treatment.

TABLE OF CONTENT

LIST OF FIGURES:

List of Tables

Chapter-1

Introduction

Nonferrous materials, like magnesium, aluminium and titanium, are used in a large scale of technical applications. They're all being considerd as steel alternatives in structural and industrial applications. (A.H. Musfirah, 2012)

The lightest structural metals in their corresponding categories are Mg alloys. They have an excellent combination of engineering characteristics, including stiffness and high specific strength. (M. Greger, 2007) because of its low density, its high strength, castability, great machinability, great weldability, remarkable damping capabilities, and ease of use, Mg alloys exhibit sparked attention as the lightest structural materials. (Robson, 2008)

Because of all of these appealing properties, the use of magnesium for structural applications would have a direct and immediate impact on areas like car fuel economy and aerospace applications. (A.H. Musfirah, 2012)

Manufacturers will be able to lower fuel consumption from an average of 10 liters per 100 kilometers to 4 liters per 100 kilometers by using Mg alloys up to 30% of total weight, or they are able to convert to other green options like electrical power, which can go 170 kilometers on a single charge.

Development of lightweight materials based on Mg is thus a crucial topic that can be significant in a variety of future engineering applications.

When good plastic deformability is required, Mg alloys become far more useful. This is a difficult restriction because to the varied property bases of Mg alloys. Because of its HCP crystal structure, Mg has a very high resistance to plastic deformation, which make it difficult to shape Mg alloys into desired shapes. In order to make magnesium alloys more acceptable for engineering applications, various attempts have been undertaken to improve their mechanical qualities and formability. Traditional processes like as rolling, forging, extrusion, and alloying, as well as the application of severe plastic deformation (SPD), are being researched to improve the ductility (formability) of Mg and its alloys. The techniques are based on a deep understanding of the structural metallurgy of magnesium alloys and how it affects mechanical behavior. (Y. Chino, 2008)

1.1 Uses of Mg and its Alloys

Mg is the world's tenth most plentiful element. According to estimates, magnesium is contained in roughly 1.90 wt percent of the earth's crust and 0.12 weight proportion of the sea. With density of 1.7 g/cm3, magnesium is the lightest structural metal, around two-thirds that of aluminium and one-quarter that of Fe. Magnesium has a HCP crystal structure. "In the late 1600s and early 1700s, Mg sulphate, often known as Epsom salts, was one of the earliest widely used forms of Mg. Despite the fact that Joseph Black discovered magnesia in 1754, Humphrey Davy found in 1808 that magnesia was the oxide of a new metal called magnesium. After mixing dry magnesium chloride with potassium to make the metal in its pure form, it took Antoine Bussy twenty years to isolate the newly discovered element Mg. Mg may be recovered from ocean via electrolysis to form Magnesium and Cl gas, Robert Bunsen was the first to show it in 1852.

By the early twentieth century, Mg's main commercial endeavor had been created in Germany, which was followed by America throughout World War I. Magnesium was largely employed in weapon manufacture because it burns hot and rapidly. However, the Germans and then the Americans began to utilize Mg alloy is used in aircraft building and in military applications Only in 1939, during World War II, was it used, taking advantage of Mg's low density. The usage of magnesium alloys in engines and vehicle components is now being investigated by major automakers in order to minimize the weight and environmental effect of gas emissions. Mg alloys are also employed in a number of items where low weight is a benefit, such as sporting equipment. Frames for bicycles, suspension housings, portable tools, and equipment storage, and a range of other consumer items benefit from magnesium's reduced weight"[32]. As a result of electromagnetic radiation limits, Mg alloys have been employed in mobile phones, cameras, and computers due to their extraordinary electromagnetic radiation resistance.

1.2 Structure of Mg alloys

Based on their production methods, magnesium alloys are separated into wrought Mg alloys and cast Mg alloys for engineering research and analysis. Die cast magnesium alloys and different casting methods have been employed in industrial applications for decades. (Kenneth Kanayo Alaneme, 2017) Apart from their commercial success, die cast magnesium alloys are only used in when mechanical characteristics and thermal stability are required in modest amounts. Wrought Mg alloys, in contrast to cast magnesium alloys, have greater mechanical properties due to their homogeneous composition and evident grain refinement free of pores. Wrought magnesium alloys offer exceptional properties that make them ideal for window and seat frames. Wrought Mg alloys are limited in their application because to their weak ductility and formability, which is caused by their HCP crystal structure and low SFE.

Mg has a hexagonal close-packed (HCP) crystal structure with weak symmetry, which is common among metals of this type. At room temperature, Mg have lattice parameters of a = 3.180 and c = 5.190, and the c/a ratio is 1.623, which is close to the optimum c/a ratio of 1.633 for HCP structures. As a result, Mg alloys have a greater primitive cell capacity than other HCP metals, resulting in lower stacking fault energy levels. (Kaya, 2013)

Stacking fault energy is the energy per unit area of the faults. A stacking fault is kind of a defect in a crystal structure that develops when atomic layers are added or removed from a series of atomic arrangements inside the crystal structure. SFE levels inside the metal govern deformation activation energies, hence it might be a helpful measure for characterizing deformation mechanisms in a very metal.

“The SFE in metals varies from atomic plane to atomic plane and is determined by dislocation configuration, native defect presence, and grain size. Low SFE favours twin deformation by raising the activation energies for slip, whereas high SFE favours slip by reducing the activation energies for dislocation movement. As a result, the low SFE of Mg alloys may play a role in his restricted ductility.

Furthermore, whereas each HCP structure has around six separate slip systems, out of six only two of them are oriented in a way that promotes slip movement.

“a [0001] <11–20>, a [10–01] <11–20>, a [10–11] <11–20>, c + a [11–22] <11–23>, c [10–10] <0001>, and c [11–20] <0001> are examples of slip systems.” (Kenneth Kanayo Alaneme, 2017)

Strain accommodation is problematic in this crystal structure due to the low symmetry of the HCP lattice, resulting in a limited range of directions for slip movement and crystallographic planes”[15].

To summarize, the c/a ratio, available deformation modes, CRSS value of slip and twin, and crystallographic textures all impact deformation processes in HCP metals. (Z. Ding, 2018)

1.3 Deformation Modes in Magnesium Alloys

“The electrical structure of materials controls their strength and resistance to various types of deformation, and it is now known that faults or dislocations in the crystal lattice generate these variations. Dislocations are often observed and studied, and their formal characteristics are well recognized. Material deformation may now be studied at several levels, including macro processes like slip or glide, twinning, and grain boundary movements, as well as the dislocation motions that support these phenomena. Because dislocations are difficult to control and manage, deformation phenomena are studied as much as possible at the macro level. Magnesium has a notable increase in flexibility when heated to 200-225°C.

According to studies, when the hexagonally crystal basal planes formations are oriented favorably in relation to the direction of tension, slip occurs swiftly up to 225°C. [11-20] is the most prevalent direction of slide that affects the basal plane. At normal temperature, magnesium deforms by twinning, in which a piece of the crystal reorients slightly to become the structural mirror image of rest as reflected on a crystallographic plane, generally the one separating the twins. With Mg at standard temperatures”[32], twinning on the pyramidal [10-12] planes happen fast. Only compression with pressures parallel to the basal planes (0001) and tension with strains perpendicular to the basal planes (0002) may achieve this form of twinning (0002). The fact that Mg's c/a value is less than a 3 / 2 is typically the cause of this. Maximum twinning occurs when the dual planes are close to 45 degrees from the stress axis. Narrow bands of twins in the [30-34] plane, which are the consequence of [10-12] twins re-twinning, are one kind of twinning that happens in Mg in small amounts. Another sort of double twinning happens in the new orientation on [10-13] followed by [10-12]. (Polmear, 2005)

Above 220°C, more pyramidal slip planes [10-11] become active. “These may function at normal temperatures in single crystals with basal surfaces positioned 6 degrees away from the stress axis, making them unfavorable for basal slip. Prismatic slip [10-10] can also happen at very low temperatures (-190°C) owing to stresses at grain boundaries that grain boundary shearing cannot relieve. Pyramidal sliding [11-22] can also happen at lower temperatures. Prismatic slip is frequent at liquid Helium temperatures. There is some indication that pyramidal and prismatic slip might alternate in wavy slip bands seen at 260° at modest strain rates. RSS on the basal plane is maximum when the basal planes are inclined at 45° to the strain axis, and it vanishes if they are parallel or perpendicular to it. It goes without saying that ductility in a polycrystalline specimen at room temperature is determined by the textural direction, which rises as grain size decreases for random orientation. Significant stresses should form at grain boundaries between grains that are unfavorably oriented for slip and adjacent grains where slip would occur quickly during deformation of polycrystalline material, and as a result, the tensile properties of Mg alloys should improve more quickly with decreasing grain size than in cubic metals, where additional modes of tensile failure exist”[32]. The allowable forms of deformation of individual grains dictate a bicrystal's malleability; hence, if one grain is oriented in such a manner that neither slip nor twinning is conceivable, the bicrystal's plasticity is zero. The fracture strain is somewhat larger when twinning is done in one grain than when twinning is performed in two grains. Following the aggregation of edge dislocations, cracking occurs around the grain boundary, where slip can occur in each crystal. The availability of higher-temperature slip planes should result in a significant rise in the tensile plasticity of polycrystalline magnesium. During tensile testing, however, such an increase in ductility is only seen in coarsely crystalline materials, and fine grain seems to “smooth out” the “expected inflexions in the temperature – strain curve. Because of the small grain size, the temperature – strain curve is likewise pushed to the left, thus steepening begins at lower temperatures.

In distorted Mg, twins and slide bands are immediately obvious. Other phenomena to consider include the following:

. Grain boundaries are tightly adhered, with evidence of deformation inside joining grains.

. Grain boundary shifts, most likely include shear and migration changes.

. Grain boundary sliding.

. Grain rotation is plainly the inverse of the preceding.

. Sub-grain formation.

. Cavitation at grain boundaries.

. Preferential orientation and compression banding are examples of textural effects”[32].

Chapter.2

Literature Review

2.1 Plastic Deformation: Basal slip:

According to (Burke E.C, 1952), “the most common deformation mode in Mg is basal slip. Basal slip dominates deformation when the basal plane is between 6 and 72 degrees from the tensile direction. They also observed that when the basal plane is perpendicular to the tensile axis, twin deformation is the most active, but when the basal plane is parallel to the tensile axis, pyramidal slip is the most favorable deformation process. Basal slip produces two separate slip vectors, permitting deformation in the closed packed plane perpendicular to the c-axis of the hexagonal lattice. The crystals had critical resolved shear stress values (CRSS) in the range of 0.50–1.50 MPa for a basal slip system sixteen. The simpler one would be activated first during deformation. As a result, in many cases, plastic deformation is dominated by basal slip” (Burke E.C, 1952). A large number of basal dislocations may frequently be found inside the deformed microstructure.

(Burke E.C, 1952), and (Hirsch et al., 1965), investigated the basal slip mode in Mg single crystals at room temperature. The work hardening behavior of Mg single crystals oriented for basal slip at various temperatures was recently published by (B. Bhattacharya, 2011). All showed two phases of the deformation process.

The long easy glide stage, also known as stage A. The work hardening rate is roughly 2 ×10-5, which is the shear modulus of magnesium, which is roughly 16 GPa. Many dislocation sources are active at the same time during this stage, and the dislocations emitted from these sources collide, forming dipole bands for each edge and screw dislocation. The screw dislocations cross glide and vanish, leaving just the edge dislocations and the screw dislocation component of the sign. Because of the dislocation annihilation, the rate of work hardening is slow at this stage. Because dislocations and mobile dislocations had very small interaction radii, their impact to work hardening is minimal. As a result, the flow stress in stage A is controlled by the inner stress field created by edge dislocations, screw dislocations, and non-primary dislocations. Dislocations glide easily at this stage. Step B is a stage of rapid hardening that is terminated by failure. The rate of work hardening at this stage is approximately 5 ×10-5. The enhanced hardening rate may be linked to the formation of dislocation tangles and a stronger dislocation network. Three types of dislocations with different Burgers vectors interact within the basal plane. Each one is at a 120-degree angle to the other. When non-primary dislocations glide across the basal plane, hexagonal networks emerge as a result. Some people also had reported the formation of deformation twins during this time, which could indicate a high work hardening rate.

2.2 Plastic Deformation: Non-basal slip:

The major slip mechanism in Mg is basal slip, which may be accomplished by two different slip systems, as previously discussed. To fulfil the Von-Mises criteria for polycrystal deformation and to explain the relatively excellent ductility of polycrystalline Mg alloys, non-basal slip should be considered. The non-basal slip mode should be able to manage the strain change on the c-axis because basal slip does not produce it. For magnesium polycrystals to exhibit good ductility, strain on the [c]-axis is necessary, especially in compression (Groves G.W, 1963)

2.2.1 c+a slip:

The most important deformation mode in Mg is c+a slip, which causes strain over both the a and c axes. Within plastic deformation of polycrystalline Mg and similar alloys, the secondary pyramidal slip (1122) <11-23> has been discovered to play an important role (Agnew S.R, 2002). (Stohr J.F, 1972) investigated this secondary pyramidal slip system in Mg in compression on the c axis, while Ando et al., 1972 investigated it in tension on the <11-20 > direction (2000 (Obara T, 1973). observed that (1122) <11-23 > c+a slip is the dominant slip mode in Mg throughout a wide temperature range when compression force is exerted on the [c]axis. Work hardening occurs at a much faster rate than basal slip.

Recent simulations have indicated that if they're seen as zonal dislocations that cause shear with both a and c components, they play an equivalent role in the nucleation and development of deformation twins. However, because each individual slip system should have its own distinct dislocation source, defining the source and operation mechanisms for c+a slip becomes a critical challenge that brings the validity of the five-independent c+a slip systems into doubt. There have been several attempts to resolve these issues. For non-basal c+a slip mode dislocations, (Yoo M H, 2001). Proposed an attractive connection between glissile a and sessile c dislocations from the prismatic plane into the pyramidal plane as a probable source mechanism. One plausible source mechanism for c+a dislocations of a pyramidal slip system.

The cross slip of a [a] dislocation from the basal plane to the prismatic plane is a crucial phase in this process. A c+a dislocation junction can form if an active prismatic slip dislocation interacts with a sessile c dislocation in a screw position. The [c] dislocation is accounted for as a pre-existing dislocation in the prismatic plane material in this case. From the (1010) plane to the (1122) plane, the screw dislocation suffers a 20th cross slip. There is no resolved shear stress to help cross slip from the basal plane to the prismatic plane since the c/a magnitude relationship for Mg is 1.6240. As a result, an attractive force should exist between a [c] dislocation on the prismatic plane and the basal [a] dislocation, causing the [a] dislocation to be pulled out of the plane. However, because c+a slips in the [11-22] plane with a slip direction of <1123 > are associated to the highest Burgers vector and hence the shortest interplanar spacing, they are often important in plastic deformation following [a] and [c] slide, making it difficult to separate the c+a dislocation activities through an experiment. As a result, direct testing is still lacking. Because of the large Burgers vector, [c+a] dislocations may dissociate. Frank and colleagues suggested dissociating a c+a type dislocation into two partials of sort <20-23>. (Frank F.C, 1953). To investigate the core structure of various dislocations, atomistic simulations of HCP metals. (Minonishi Y, 1986). Documented the separation of this type of dislocation.

They proposed two distinct types of dissociations. The first occurred due to a stacking defect, which resulted in the dissociation of a c+a dislocation into two c+a kinds of dislocations in the [11-22] glide plane, which may be described as:

$$\frac{1}{3}[11\bar{2}3] + \frac{\eta}{3}[11\bar{2}3] + \frac{1-\eta}{3}[11\bar{2}3] + \text{SF}\ (11\overline{22})$$

The other was a stacking defect within the basal plane that split a [c+a] dislocation into 1/3[$10\bar{1}0$] and 1/3[$01\bar{1}3$] type dislocations.

Dissociation of a [c+a] dislocation into a [a] dislocation and a [c] dislocation is also possible.

2.2.2 Prismatic Slip:

In HCP Mg, Prismatic Slip [1100] <11-20> may also be detected. The first order prismatic slip works at room temperature in Mg with the loading direction parallel to the basal plane, especially at the grain boundaries' corners, as discovered by Reed-Hill et al., and Ward Flynn et al. Pyramidal slip on (10-11) would occur at a higher temperature because prismatic a slip cannot create strain on the c axis.

The CRSS for the first order prismatic [a] -slip at ambient temperature is roughly 45 MPa. The CRSS for prismatic slip in Mg is temperature dependent, according to (Couret A, 1985). In comparison to basal slip, the dislocation core on the prismatic plane is metastable due to the significant stacking defects energy (Couret A, 1985)

Prismatic c -slip is theoretically feasible as well. The Burgers vector for c dislocations is in the [0001] direction. They'll apply pressure on the c axis. Due to the substantial general stacking fault energy needed, which directly restricts the mobility of dislocations in Mg, the prismatic c slip is seldom encountered experimentally. c dislocations, on the other hand, have been discovered in a number of studies. (S. Morozumi, 1976). investigated the dislocation structure of Mg alloy using TEM. Many - dislocations were discovered, notably at the grain boundary regime.

2.3 Plastic Deformation: Deformation twinning:

Basal slip is the most active slip mechanism in Mg, as previously indicated, although it cannot induce strain change on the c axis. As a result, twinning deformation in Mg is the most prominent deformation mode at room temperature. The length-to-thickness ratio of these animals is generally fairly high. The tip of the twin is in the shape of a lens, where a large density of dislocations is formed due to the high local-stress concentration. Dislocation density is frequently higher in the twin than in the matrix. Little twin embryos can be observed when the strain is less than 5-hitter.

The size-related twin behavior of HCP materials differs significantly from that of FCC metals. Within the coarse-grain size range, deforming FCC metals by twin becomes progressively difficult; yet, if the grain size is lower than 100 nm, twin becomes simpler; yet, twin may become difficult once the grain size is just too tiny.

The corresponding size regime is generally 5-10 nm, where the deformation twin fades once more. Due to a lack of appropriate slip systems, coarse-grained HCP metals usually require twin to allow both plastic deformation and dislocation slip. Due to the decrease in grain size to roughly 100 nm, twin is unusual in nanocrystalline Mg. The tremendous energy of stacking faults might be one of the explanations. When the stacking defects energy is reduced by creating alloy, deformation twinning occurs in nanocrystalline Mg-9.50 at. percent Ti alloy, according to Wu et al.

(Qian Yu, 2010). Report a significant crystal size discovery in a single crystal HCP Ti deformation twin. On Ti alloy, state-of-the-art in situ Transmission electron microscopy and nanomechanical testing were used to study spatial-temporal correlations and the influence of sample size on deformation twin. When the sample diameter was reduced to less than 1m, deformation twin went away and was replaced by normal dislocation plasticity, a mechanical transition that is easily accessible in practice. Furthermore, the materials' strength appeared to saturate in lockstep with the deformation mechanism switch. Deformation twinning-induced strain bursts are usually replaced by continuous plastic flow at theoretical high-level stress by simply lowering the sample diameter, a characteristic that is extremely desirable for plastic forming and structural applications.

2.4 Mechanical Properties:

2.4.1 Strength and ductility:

(Kelley E.W, 1968). Investigated a series of single crystal Mg orienting from

1 to 7 using channel-die compression experiments (see Table 1 for orientations). During single crystal testing, multiple deformation modes were used depending on the specimen orientations. This makes it possible to determine the hardening parameters for a certain slip mechanism.

Table 1.Several orientations used in channel-die compression studies on single crystals in (Kelley E.W, 1968)

Test	Loading	Constraints
1	(0001)	[10-10]
2	(0001)	[1-210]
3	$(10\bar{1}0)$	[0001]
4	(1210)	[0001]
5	$(10\bar{1}0)$	[1-210]
6	(1210)	[10-10]
7	(0001) at 45	[10-10]

According to the microstructure analysis, only curves A and B show more than one family of slip mechanisms working at the same time, notably prismatic and pyramidal slip. Prismatic slip dominates curves C and D across the whole range of strain, while basal slip dominates curve G. For orientations E and F, the transition from twin to pyramidal slip happens across a very narrow range of stress. Twin deformation is encouraged in orientations E and F, resulting in a c-axis elongation. Because of its low CRSS, tensile twin is certainly triggered; elastic deformation will rise stresses until they approach the CRSS of pyramidal glide, causing a rapid rise in stresses at around 0.060 strain.

They also investigated the mechanical characteristics of polycrystalline Mg using different texturing techniques. Prismatic slip induces about an hour of plastic deformation within the specimens of orientations LT and tl, with yield strength of about 30 MPa and peak flow stress of about 155 MPa. In specimens with orientations sl and ST, pyramidal slip predominates, with yield strengths of approximately 40 MPa and peak flow stresses of roughly 265 MPa. Basal and prismatic slip contribute almost equally by approximately 400th, while prismatic slip contributes nearly equally by approximately 200th. Low yield strength and hardening for the orientations TS and LS result from the activation of tensile twin (CRSS at about 5 MPa), which contributes to plastic deformation by about 400th, and the rapid increase in stresses exceeding 5-hitter strain arises from the saturation of twin and the additional activation of pyramidal slip.

2.4.2 Elastic properties:

When a force is applied, the modulus of elasticity is a mathematical representation of an object's or substance's tendency to deform elastically. The elastic modulus of an item may be calculated using the slope of its stress–strain curve inside the elastic deformation region. The elastic properties of single crystal Mg alter with various crystal orientations due to its anisotropic nature. (Slutsky et al.) tested the elastic constants of pure Mg at temperatures ranging from 4.20K to 305K using an ultrasonic pulse method. At room temperature, Young's modulus is roughly 46 GPA.

2.5 Size effect:

Materials' mechanical characteristics might vary depending on their interior and exterior dimensions. In most cases, the sample size determines the exterior dimension. Grain sizes are generally used to calculate internal dimensions. The internal dimension can also be tuned using phase and twin boundaries. As previously said, material yield strength is defined as the stress at which a specific amount of permanent deformation occurs, which is the word that is directly related with the movement of dislocations. Dislocation actions can occasionally influence the plasticity of materials. Each one is proportional to its size.

2.5.1 Internal-Dimension Refinement-Grain Boundary Strengthening:

When the stress reaches the dislocation's Critical Resolved Shear Stress, the dislocation begins to move. Dislocation propagation is prevented by the grain boundaries acting as pinning sites. Because the orientation of neighboring grains vary, "it takes a lot of energy for a dislocation to change directions and travel into the next grain. The grain border is also significantly more disordered than the grain interior, which prevents dislocations from migrating on a continuous slip plane. As a result, preventing dislocation motion can delay the onset of plasticity and therefore enhance the material's yield strength."[31]

"The specifics are shown below. Pre-existing dislocations and dislocations created by Frank–Read Sources can migrate across a crystalline lattice until they reach a grain boundary, where the massive atomic mismatches between the various grains form a repulsive stress field that prevents further dislocation motion. As more dislocations propagate to this barrier, dislocations build up, making it difficult for them to go past it. Every subsequent dislocation might apply a repulsive force to the prior dislocation against the grain boundary because dislocations create repulsive stress fields. These repulsive forces will function as a driving factor to lower the energy barrier for diffusion across the boundary; further, pile up produces dislocation diffusion over the grain boundary, allowing for more material deformation. Reduced grain size reduces the amount of possible pile up at the grain border, increasing the amount of applied stress required to move a dislocation over it. As a result, materials with smaller grains will be more durable. The Hall–Petch equation is a good example of this."[31]

$$\sigma = \sigma 0 + kd^{-0.5}$$

σ is the yield strength, k is a constant and d is the grain size.

Experiments have shown that the Hall–Petch relation is a good model for materials with grain sizes ranging from 1 mm to 1 micrometer. Experiments on numerous nanocrystalline materials, on the other hand, showed that if the grain size was reduced to a threshold value, generally less than 100 nm, the yield strength remained constant or decreased as grain size decreased. The inverse Hall–Petch connection is the term given to this relationship. Several theories have been presented as to why the Hall-petch to inverse Hall-petch effect related transition occurs. The main problem is that dislocation activity in extremely tiny grains would be difficult to generate, allowing alternative deformation modes, such as grain boundary sliding or grain rotation, to take over and dominate the plastic deformation. As a result, strain softening rather than strain hardening may occur. Low sample quality and the suppressing of dislocation pileups are among the several hypotheses given to explain the apparent softening of metals with submicron grains.

2.5.2 External dimension refinement:

The exterior geometry of materials can have an impact on their strength and physical properties. For example, near-ideal material strength was achieved in micron-sized single-crystal metallic whiskers, albeit at the expense of plasticity.

The size effects are expected to be explained by a dislocation-source truncation process and exhausted hardening methods. It is hypothesized that the length of a free arm dislocation source is directly governed by the sample dimension since the sample dimension drops to the same order as line defects, resulting in L D, where L is the length of the dislocation source, D is the sample dimension, and is a positive integer. The critic resolved shear stress for a dislocation source is inversely related to its length, as shown by the principle of size result, which can be stated as $\boldsymbol{\sigma}$=Gb / L, where $\boldsymbol{\sigma}$ is the CRSS, G is the shear modulus, and b is the Burgers vector. Because the length of a dislocation is controlled by the sample's exterior dimension, a smaller sample size might shorten the dislocation source, resulting in a higher CRSS. The most important notion in the exhaustion hardening process is also the size-related functioning of the dislocation source. It has been established that when deformed, the main dislocation source in a very small volume may begin to act initially, but rapidly become "exhausted," necessitating the use of the secondary dislocation source, which requires higher stress. This effect becomes much more prominent when the exterior dimension of the specimen is reduced to the micron scale, and it is usually referred to as "smaller is stronger." Although the GPa rate strength is exciting for application, the precise characterizations on materials' ability of plastic deformation still want further investigation to develop the comprehension on the size-related plastic behavior of materiel.

Microstructure is very important for the mechanical characteristics of materials. As previously stated, dislocation activities and, as a result, the functioning of the Frank-Read source directly validate the strength and ductility of materials. Because prior ex situ investigations were unable to give temporal information during plastic deformation, a significant amount of work is required to determine the relationship between microstructure evolution and, as a result, size-related mechanical response of materials.

2.6 Enhancing Deformability of Mg Alloys:

There are several ways to improve the deformability of Magnesium alloys and these ways are reducing the c/a ratio, modify the texture, grain refinement and activation of the non-basal slip mode. This all will be done by adding an alloying element, using several plastic deformation techniques.

2.6.1 Alloying:

This is the basic method for improving the deformability of magnesium alloy. Numerous investigations have revealed that adding alloying elements in Mg alloys improves deformability by narrowing the CRSS gap "between slip modes and affecting twin response among grains during deformation. Rare Earth elements have been shown to alter the crystallographic texture of Mg alloys by promoting non-basal slip mode during deformation, slowing dynamic recovery and recrystallization processes, and encouraging the growth of non-basal oriented grains.

Mg alloys are divided into several series according on their alloying elements, with the most common being AZ, AM, AE, EZ, ZK, and WE. In the Mg alloy series, two numbers reflect the content of each element present in the alloy in the order they occur in the percentage composition of the alloying components"[15]. For example, AZ31 signifies a 3 percent Al,1 percent Zn alloy, whereas a zero represents any element having a composition of less than 1%. (Kenneth Kanayo Alaneme, 2017)

2.6.1.1 Mg-Al System:

Adding aluminium enhance the mechanical properties like strength, plasticity of Mg alloys, Most extensively utilized material as an Magnesium alloy are Mg-Al based alloys. Mg17Al12 phase formed on grain boundaries, on the other hand, it has a low melting temperature (550˚C), causing microstructure instability above 395 K. At high temperatures, this causes grain boundary sliding and, as a result, a decrease in the mechanical properties of Mg-Al alloys. Furthermore, during the rolling plasticity of Mg-Al alloys at ambient temperature is limited by a strong basal texture, and nonhomogeneous grain sizes. In order to improve the microstructure of Mg-Al alloys, a variety of elements were used. "Mg-Al-Zn, Mg-Al-Mn, and Mg-Al-Si have all been mostly used because Zinc enhance mechanical properties of Mg-Al alloys at low temperatures and Mn and Si improve creep resistance. In addition, within the last decade, the addition of Cadmium, Lithium, Strontium, Tin, Rare Earth and other elements to commercial Mg-Al system alloys has been thoroughly investigated. When Cadmium is added to Mg-Al alloys, a thermally stable Al2Ca phase with a higher melting temperature of 1050˚C can emerge, which could improve the mechanical properties of Mg-Al alloys significantly. By adding 1.70 wt. percent Ca, increases the UTS, yield strength, as well as elongation of extruded Mg-2.320Al alloys to 320 MPa, 271 MPa, and 10.20 percent, respectively. The effect of adding Cadmium to Mg-Al alloy"[33] ensue exceptional grain size reduction, and the production of 35-55 nm plate-like Al2Ca molecules accumulated within grains all of which resulted in a good mechanical property. When a Ca-containing AZ31 alloy was thermo-mechanically treated, the results were similar, with finer grains and better ductility than the Ca- free AZ31 alloy. GB distribution and texture, on the other hand, was identical. Kwak et al found that the hot compression behavior of the extruded AZ31-Ca alloy containing 0.5 wt.% Ca, and discovered that the addition of Cadmium resulted in reduce in grain size and microstructure that is homogenous. In addition, when comparison with the extruded cadmium "free AZ31 alloy, the extruded 0.50 wt. percent AZ31-0.5Ca alloy have good plasticity at high temperatures (575–675 K) but worse plasticity at low temperatures. The reason behind that at high temperatures, the Al2Ca phase disperses within the matrix, promoting dynamic recrystallization and delaying grain coarsening. At varied temperatures and strain rates, adding Cadmium, Strontium, and Cerium to the

AZ31 alloy had no effect on the deformation process., but it did have a noticeable impact on the alloy's ductility at high temperatures and low strain rates; under these conditions, the elongation to failure increased from 350 percent to 400 percent, and 430 percent. The results revealed that adding Ca, Sr, and Ce to the mix decreased grain coarsening and hence enhanced plasticity during hot deformation.

Because in Mg alloys, Li's lower density encourage the cross-slip and non-basal slip modes, it is another plausible ingredient to enhancing the microstructure of Mg-Al alloy. Pan's Chongqing University research group has done a lot of work on the mechanical characteristics and deformation behavior of shaped AZ31-xLi alloys, and these studies are very useful. It was discovered that Lithium has a very good solubility in Magnesium alloy, implying that Li might significantly modify the lattice characteristics of Mg solid solutions, as shown in Table 2. As a consequence, with increasing Lithium content, the c/a ratio of the AZ31 alloy was dramatically decrease. Furthermore, As lithium amount is increasing basal plane poles rotation in the TD, decrease the intensity of the basal plane texture which is present in extruded AZ31, and randomized grain boundary orientation distribution . The enhanced ductility and decreased anisotropy of AZ31 alloy were ascribed to the changed texture, lower c/a ratio price, and decreased grain size induced through the Lithium addition.

Table 2: Mg solid solution lattice parameters (Y. Zeng, 2015)

Alloy	a (Å) Volume (Å3)	c (Å)	c/a	Volume (Å3)
AZ31	3.20440 ± 0.0020	5.20550 ± 0.004	1.62450 ± 0.001	46.290
AZ31-1Li	3.19900 ± 0.0040	5.18760 ± 0.0060	1.62160 ± 0.0020	45.970
AZ31-3Li	3.19340 ± 0.0040	5.14870 ± 0.0020	1.6170 ± 0.0020	45.470

AZ31-5Li	3.18640 ± 0.0040	5.12780 ± 0.0040	1.60820 ± 0.0010	45.090

2.6.1.2 AM series:

AM50 and AM60 are Mg-Al-Mn-based alloys that have a good mix of strength, plasticity, and corrosion resistance, and are broadly employed in applications that need a lot of plasticity and toughness, incorporating instrument and navigation controls. Though, owing to poor higher temperature mechanical characteristics produced by the precipitation and coarsening of the Mg17Al12 phase in the Interdimeric eutectic region, AM series alloys have a maximum application temperature of 115 °C. In this example, the addition of numerous alloying elements to AM series alloys was examined in order to advance their mechanical characteristics at high temperatures and increase the usage of Magnesium alloys.

Addition of RE element to AM series alloys is an effective technique to improve their mechanical characteristics. He et al discovered that the La/Ce ratio has an effect on the microstructure and mechanical characteristics of AM50-1RE alloys with constant Rare earth concentration (1.20wt percent). AM50-1La alloy provides a better strengthening effect than Cerium due to its fine grain size”[33]. However, combining Lanthanum and Cerium results in the loss of Mg17Al12 phase and the production of coarse skeleton-like phase, thus la has a stronger strengthening effect than Cerium.

2.6.1.3 Addition of RE:

For the increase of wrought Mg alloys' strength and formability, Mg wrought alloys incorporating multiple RE elements have piqued attention. RE additions have been discovered to significantly degrade the texture and increase the plasticity of Magnesium alloy, according to extensive study. Because of their great solubility in Mg, REs may efficiently strengthen Magnesium alloy through solid solution strengthening and precipitation hardening methods. Wrought magnesium alloys containing rare earth elements including Gadolinium, Yttrium, Neodymium, Dysprosium, Holmium, Erbium, Cerium, Lanthanum, and Ytterbium have recently been created. At both ambient and higher temperatures, the binary and ternary Mg-RE alloys show high strength.

2.6.2 SEVERE PLASTIC DEFORMATION (SPD) TECHNIQUES:

The traditional forming processes are limited to improvement of formability of Mg alloy at high temperature because of this there is need to find out other more impactful processing techniques which can improve the formability in Mg alloy hence severe plastic deformation techniques comes in the picture of Mg alloy processing at room as well as high temperatures.

“In severe plastic deformation techniques there is significant improvement is recorded in terms of mechanical properties and stretch formidability at room as well as elevated temperatures.”[15]

“SPD is a well-known forming process which can introduce very high plastic strains in material which accounted b rearrangement of distorted structure (dislocation) and non-equilibrium grain boundaries which accounts for substantial grain reduction to submicron to nanoscale levels. The very ultrafine grain formed by SPD techniques causes improvement in mechanical properties which is due to the formation of high densily of internal interface like twin, grain and sub grain boundary. By these techniques also basal texture is weekend due to propensity for twinning as grain size reduces. Some famous SPD techniques are:”[15]

- Equal channel angular extrusion (ECAP/ECAE)
- High pressure torsion (HPT)
- Accumulative rolling bond (ARB)
- Multidirectional forging (MDF)
- Cyclic extrusion compression (CEC)
- Differential speed rolling (DSR)
- Accumulative back extrusion.
- Tube cyclic expansion extrusion.

2.6.2.1 Equal channel angular extrusion (ECAP):

Using ECAP, bulk ultrafine magnesium alloys can be produced with improve d material integrity and functionality without changing the dimensions of the work. High quantity of material is compressed by an angular die and plastic strain is produced without changing the dimensions of the work by feeding the workmaterial in two intersecting channels of same cross-section form the die. Shear strain is produced at their intersections, resulting in an accumulation of strains upon repeated pressing. Nevertheless, deformation process success of this process is dependent on several factors, including die shape, angle between dies, rate of pressing, number of passes, workpiece temperature. Fig represent the ECAP schematic process.

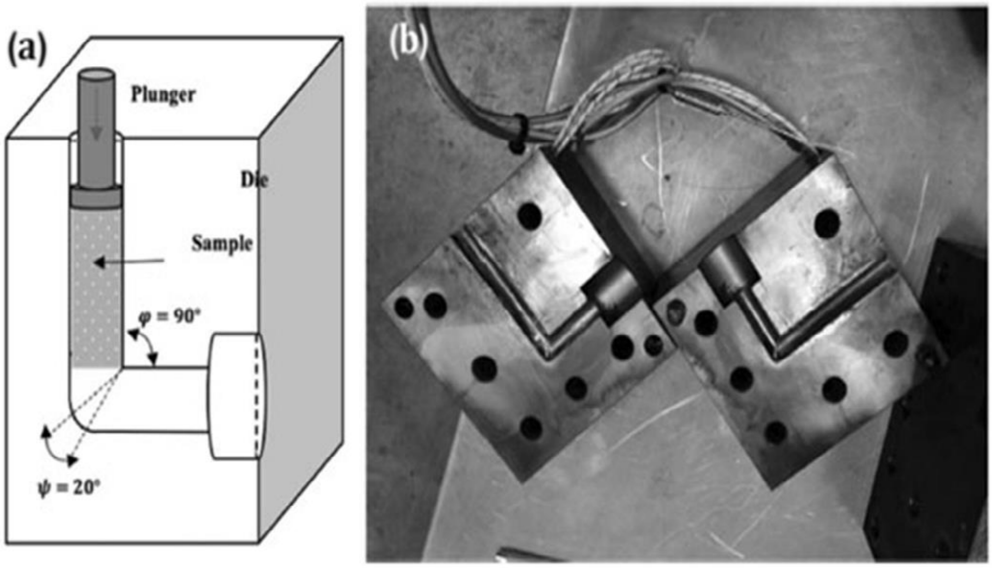

Figure 2.1 (a) Schametic of ECAP (b) pictorial representation of ECAP process (after Khani et al. , Elsevier).

"When Mg alloy is subjected to ECAP processing at elevated temperature, significant grain refinement and non-basal slip occurs in the crystal structure. As the number of ECAP deformed Mg alloy increases, it increases the degree of grain size reduction and homogeneity in grain structure."[15] Enhancing the mechanical properties of Mg alloy is associated with the refinement of grain structure in ECAP SPD process.

In the case of Mg alloys, cracking of alloys is a major issue associated with E CAP processing at low temperatures. A lack of active slip systems, in particular dislocations in non-basal slip planes, contributes to the occurrence of cracks in the alloy "at ambient temperatures, which increase the plasticity of the alloy. Because of this, ECAP processing of Mg alloys has been limited to processing at elevated temperatures and refinement has been limited due to grain growth.”[15]

2.6.2.2 High pressure torsion:

Metallic materials can use this processing method to refine grains during SPD processes, increasing the level of grain refinement. In HPT, our test material is in the disc form and are placed in between of two anvils which are apply high pressure on our test sample disc along with torsion straining by bottom anvil. Due to this applied pressure (compressive stresses) high hydrostatic forces is imposed on the material due to which a high shear strain generated on material which produces ultrafine grain of submicron to nanoscale levels.

Maybe due to High hydrostatic force, formation of crack is stopped and hence we can process our material at room temperature without crack formation in material. Due to deformation of material at room temperature there is no dynamic recrystallization or very less dynamic recrystallization in the material and hence very fine grain refinement and strain hardening of test sample is achieved.

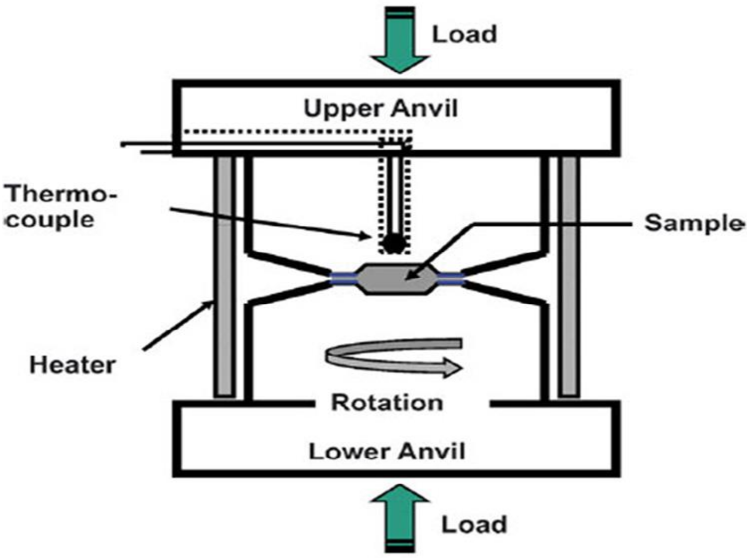

Figure 2.2 A schematic of High pressure torsion (after Kai et al.).

By the HPT process the grain refinement we achieve is greater than the ECAP process. It is proposed that atleast one turn is required to generate homogeneous microstructure in our test sample. The grain size of alloy decreases from center to periphery. It is also proposed that increase in number of turns of our test material in the HPT processing contribute in increased grain refinement and also reduces variation in grain size from center to periphery.

High temperature processing of Material in HPT process is area of concern because of dynamic recrystallization and grain growth in material. Simultaneously causes premature crack initiation at high temperature.

2.6.2.3 Accumulative roll bonding:

It is the only SPD process which is take advantages of rolling process as to induce plastic strains to help refinement of grain structure. “It is a two stage SPD technique which involve rolling (Deformation) and bonding. In this technique half rolled test material is cut into two or more parts, than collect to initial rolling dimension and rolled again. After the first pass i.e. in second rolling the two half of material joined together and make a single sheet. And so on. Fig represent the schematic of ARB process.

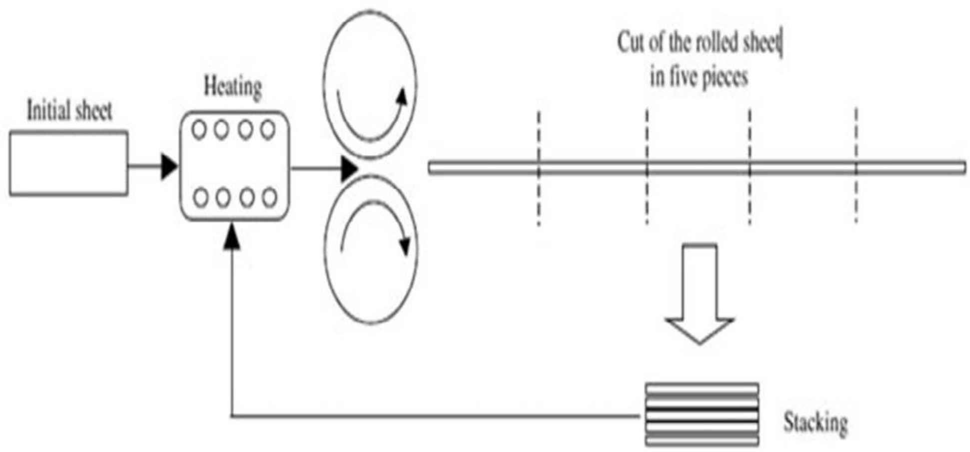

Figure 2.3 Accumulative Roll Bonding Process(after Perez-Prado et.al).

the effectiveness of this technique is depends on the temperature of rolling and the reduction of thickness per pass. The effect of high temperature and high reduction helps in bonding but lower temperature forms the smaller grain size”[15].

Chapter.3
Objective

The mechanical properties of magnesium alloys can be improved by refining the grain size to nanometer level by using non-conventional processing methods, such as equal channel angular processing and high pressure torsion. And also we know Segregation can minimize the strain associated with the grain boundaries. Hence, it is important to understand the segregation behavior in Mg alloys.

Although large amount of work done previously on Mg - Ca based alloys, the present study differs from earlier studies in the following aspects.

1. Mg - 0.4wt% Ca alloy processed by HPT was not studied earlier.

2. No systematic study was carried out to show the effect of segregation on microstructure stability. Moreover, in previous studies small precipitates were found at grain boundaries along with segregation. So, it was not clear whether grain growth was hindered by grain boundary pinning effect or segregation effect. Furthermore, in earlier studies the amount of segregation was not uniform across the boundaries.

3. In the present study, more careful experiments are designed to obtain only segregation phenomenon uniformly over the large fraction of grain boundaries. Hardly any precipitate could be observed to eliminate the grain boundary pinning effect.

Chatpter.4

Experimental Procedure

This chapter shows the experimental procedures employed in the research.in this we are going to see the effect of segregation on microstructure stability and mechanical property on Mg-0.4wt% of Ca alloy. The main microscopy techniques are used to study the deformed material is TEM (Transmission Electron Microscopy).

4.1 Materials:

In this experiment, the main matrix material is Mg and we added Ca in minimum quantity so we can get segregation uniformly across all grain boundaries in Mg- Ca binary alloy. In this alloy system we choose amount of Ca is 0.4 wt% because of if we choose 0.1, 0.2 wt% there is no segregation shown in Mg-Ca matrix. At 0.3 wt% of Ca there is segregation but not uniform throughout the matrix. At 0.4wt% of Ca we get uniform segregation throughout in matrix. If we increase the quantity of Ca it tends to form precipitates along with segregation that we don't want because our main focus is to study the effect of segregation in Mg- Ca matrix. Also extra addition of Ca amount increase the cost also.

4.2 Stir Casting:

Stir casting is the most economical technology to produce metal matrix composition like Aluminums and Magnesium. In this casting method, a stirrer is used which is placed into the liquid molten metal applies some mechanical rotation (rpm) to obtain the desired distribution of the reinforcement with the liquid molten metal.

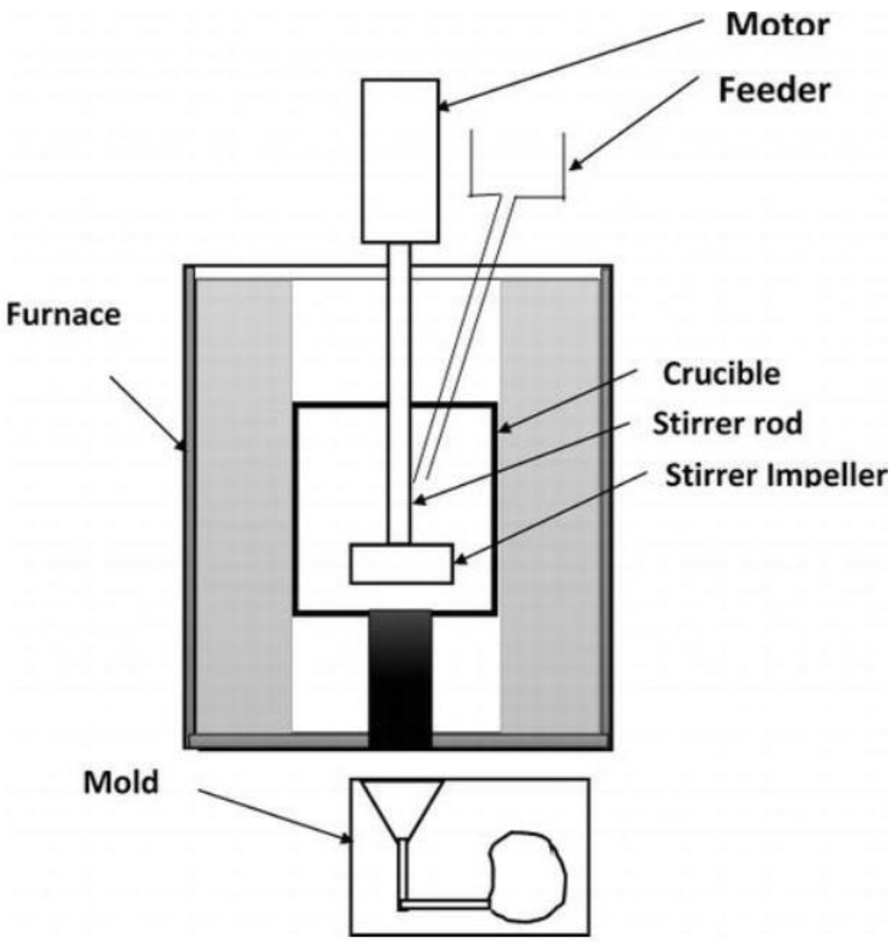

Figure 4.1 Stir Casting (Amol D. Sable, 2012)

Fig 4.1 show are schematic representation of the stir casting method. Stir casting method consist of a furnace, stirrer and reinforcement feeder. The furnace is used for heating as well as for melting the material. A stirrer is used for mixing of reinforcement with the molten metal. The motor is connected with the stirrer which is help to control the rotation of the stirrer through the regulator.

4.2.1 Procedure of Mixing

Step For the process:

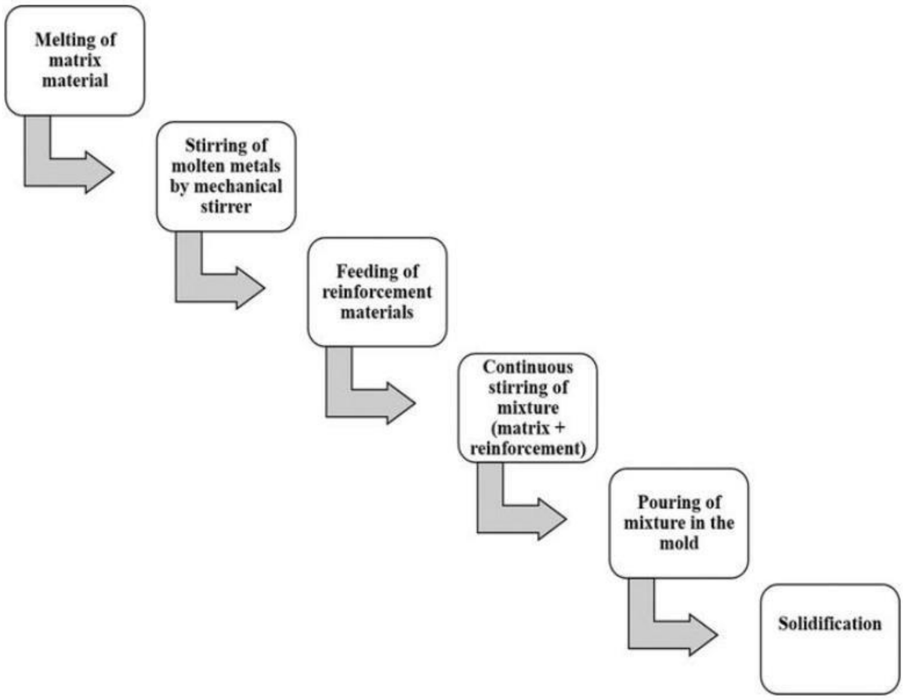

Figure 4.2 following step of stir casting (Amol D. Sable, 2012)

4.3 Extrusion:

"Extrusion is a metal forming process in which work piece is compressed to flow through a channel or die to reduce its cross section so it convert into desire shape. This process is used to manufacture pipes and steel rods. Compressive force is used to extrude the work piece. Drawing process is also look similar to extrusion but the difference is drawing process uses tensile stress to deformation in workpiece"[30]. The deformation is large in extrusion process, comparison with drawing in single pass because of compressive force used to deform material in extrusion. Plastic and aluminum is mostly extruded material.

4.3.1 Working principle:

It is a metal forming process which uses compressive forces on metal workpiece. In this process a ram or a plunger or piston is apply pressure to our workpiece. The working principal of extrusion typically follows steps which are.

- "Metal work piece of standard size is produced which is call as billet or ingot.
- This billet is heated in hot extrusion or remains at room temperature and placed into a extrusion press (Extrusion press is like a piston cylinder device in which metal is placed in cylinder and pushed by a piston. The upper portion of cylinder is fitted with die).
- Now a compressive force is applied to this part by a plunger fitted into the press which pushes the billet towards die.
- The die is small opening of required cross section. This high compressive force allow the work metal to flow through die and convert into desire shape.
- Now the extruded part remove from press and is heat treated for better mechanical properties"[30].

4.3.2 Types of extrusion:

4.3.2.1 According to direction of flow of metal

4.3.2.1.1 Direct extrusion:

This is a type of extrusion process in which work material is forced in the direction of punch by applying compressive force through plunger as seen in fig.4.3 in direct extrusion process plunger moves and die remains stationary. In Direct extrusion due to high friction between ingot or billet and container the force requirement is high.

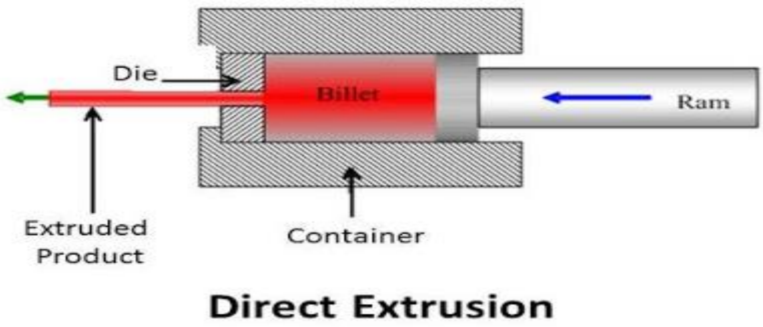

Figure 4.3 Direct extrusion

4.3.2.1.2 Indirect Extrusion:

In Indirect extrusion the punch is remains stationary and die moves hence the metal is flowing in opposite direction of punch movement. And the metal is flow in between the plunger and the die as seen in fig. 4.4

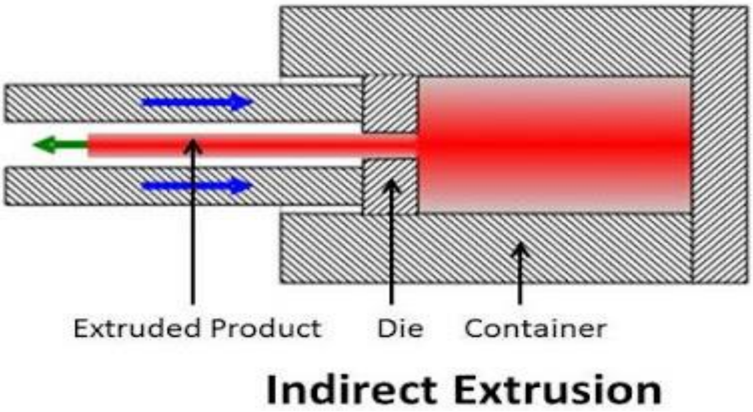

Figure 4.4 Schematic of Indirect extrusion

4.3.2.1.3 Hydrostatic Extrusion:

In hydrostatic extrusion there is a fluid in between workmaterial and punch. And this fluid apply pressure to the workmaterial. Due to using fluid the friction generated is very minimum means almost negligible because the workmaterial is not contact directly with cylindrical wall and punch as seen in fig.4.5 due to less friction less power is required for this process. The force applied by punch on fluid is transferred to the workmaterial. Normally fluid used in this process is vegetable oils. The two problem occurred in this process are 1). Leakage problem 2). Uncontrolled extrusion speed.

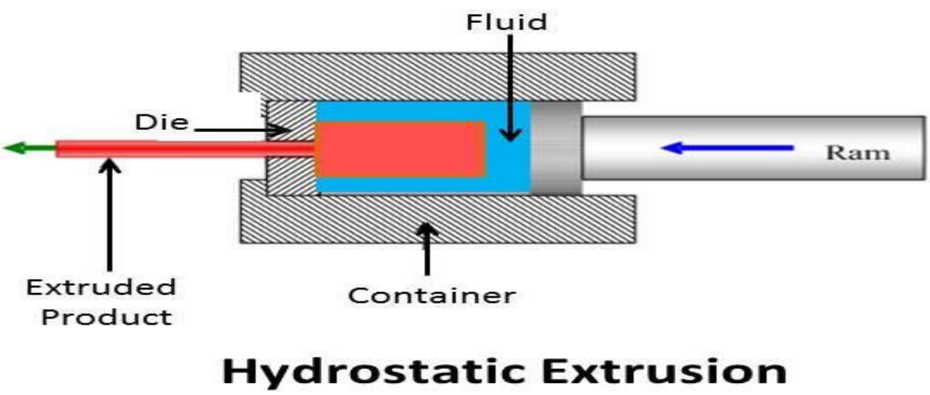

Figure 4.5 Schematic of Hydrostatic extrusion

4.3.2.2 According to working temperature:

4.3.2.2.1 Hot Extrusion:

Hot extrusion takes place above the recrystallization temperature about to 55 to 65% of melting temperature of workmaterial. The following advantages of hot extrusion process are: 1). Compared with cold extrusion less force is required. 2). Easy to deform. 3). Strain hardening is not associated with hot extrusion.

Some limitations are: 1). Due to scale formation, there is less surface finish of extruded part. 2). Die wear rate is increases. 3). Maintaince requirement is high.

4.3.2.2.2 Cold extrusion:

Cold extrusion takes place at room temperature or below recrystallization temperature. Some example of cold extrusion process are aluminum cans, collapsible tubes and cylinders etc. Advantages of cold extrusion process are: 1). Very high mechanical property obtained. 2). Very high surface finish obtained. 3). Metal surface is free from oxidation at metal surface.

Some limitations are: 1). Compared with hot extrusion high work force is required. 2). Strain hardening is associated with product.

4.4 TEM (Transmission electron microscopy)

TEM (Transmission electron microscopy) is a microscopy method in which a electrons beam is pass through an extremely thin specimen (often less than 250 nm thick) and interacts with it as it passes through. Electrons are accelerated by an electric potential as they exit the filament, which is made of tungsten. The entire system runs in a vacuum. The electrons are then focused into an extremely concentrated beam using electromagnetic lenses in the TEM.

The electron beam then passes through the sample, interacting with the structures and materials along the way. Electrons, unlike X-rays and neutrons, are charged particles that interact with matter through Coulomb forces. This indicates that both the positively charged atomic nuclei and the surrounding electrons have an impact on the incident electrons. The transmitted beam, elastically diffracted beam, and inelastically scattered electrons are formed by three separate interactions of electron beam-specimen in TEM.

The electron beam that passes through a thin specimen without interfering with it is referred to as a transmitted beam. The transmitted beam intensity is inversely proportional to the thickness of the specimen. As a result, in a bright-field TEM picture created by a transmitted beam, which means formation of the bright field image by using only the transmitted beam and formation of dark field image by using only one strong diffracted beam which means thicker portions of the specimen will have fewer transmitted electrons and seem darker. Dark Field Image and Bright Field Image is shown in Figure 4.6. The mass thickness Contrast is frequently used to produce low magnification pictures.

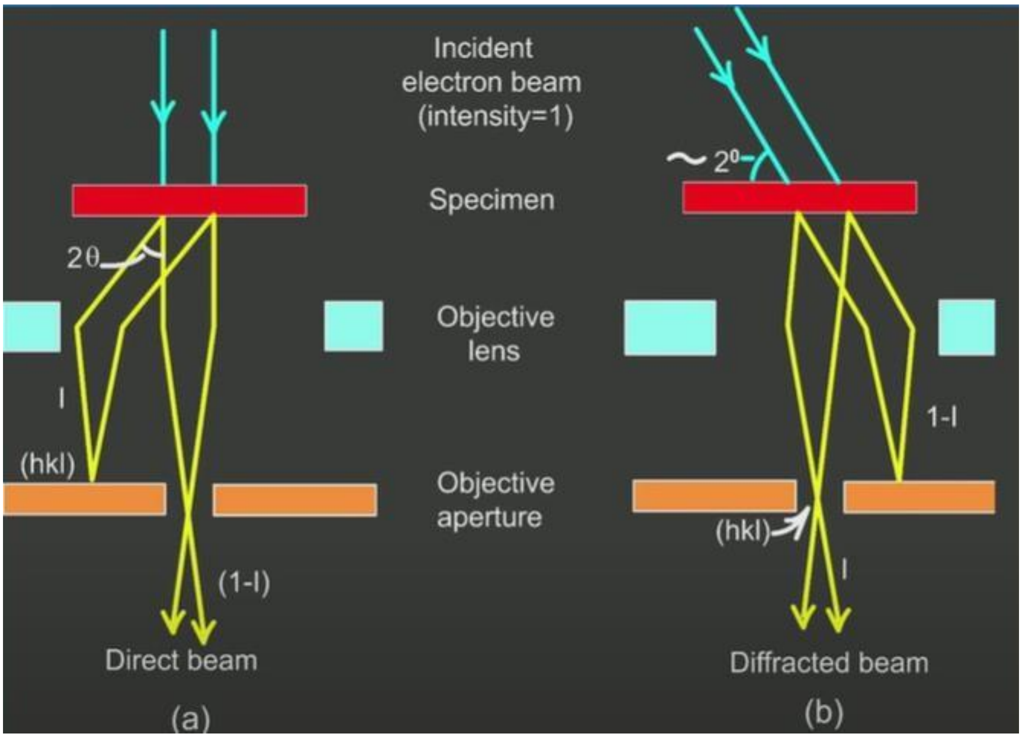

Figure 4.6. Schematic of Dark Field Image and Bright Filed Image, (Thomas, 1962)

The TEM picture is then amplified and focused on a layer of photographic film using an imaging device, such as a fluorescent screen.

Another part of the incident beam is scattered by atoms in the specimen. It is elastic scattering so that there is no loss of energy. These scattered electrons are then transmitted through the remaining portions of the specimen.

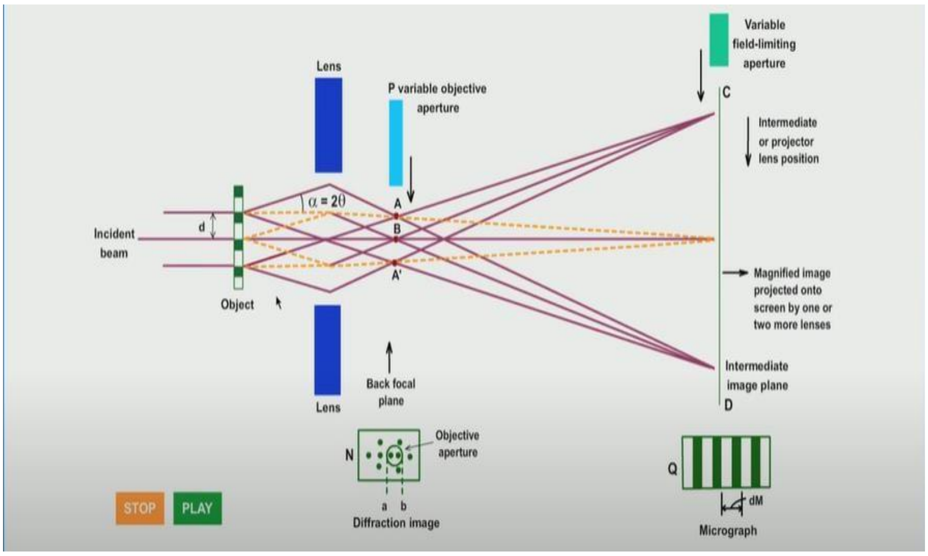

Figure 4.7 Illustration of TEM (Thomas, 1962)

The diffraction of electrons is described by Bragg's Law, which is 2d sinθ = nλ, where λ is the wavelength of the rays, θ is the angle between the incident rays and the crystal surface, and d is the distance between atom layers . As a result, all incident electrons with the same atomic spacing will scatter at the same angle.

If the d and θ fit the Bragg's law, a constructive beam can be formed. Magnetic lenses may be used to collect the dispersed electrons and produce a pattern. a number of dots, each one corresponding to a different atomic spacing. This is it. Diffraction pattern is what it's called. This pattern can then be used to deduce information about the subject. In the area under investigation, the orientation, atomic configurations, and phases are all present. As a result, Bragg contrast is used to create the image of the diffraction pattern. Furthermore, because flaws like dislocations and twinning will have an impact on the interaction the diffraction condition will vary when electrons and materials interact, therefore.

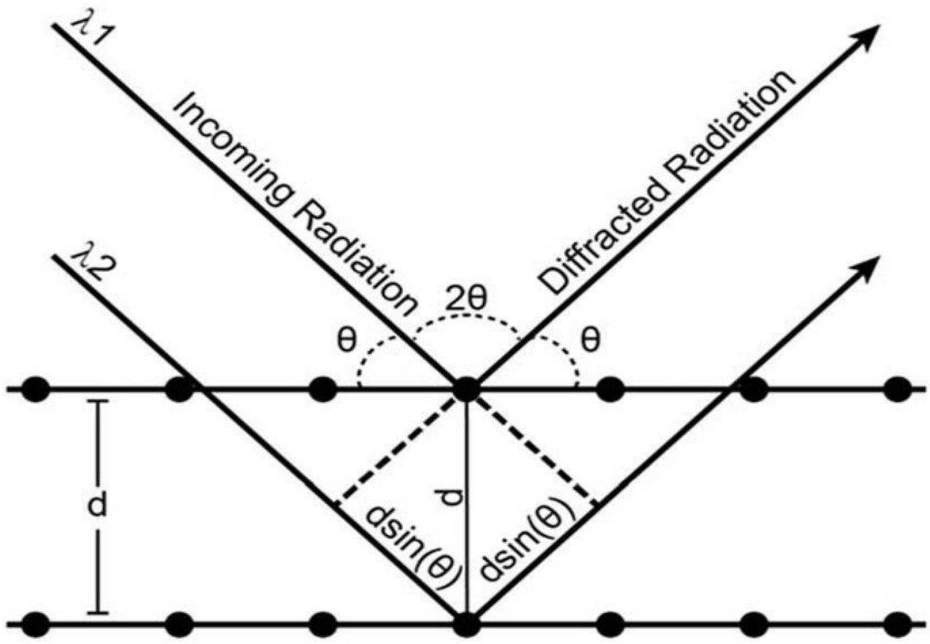

Figure 4.8 Illustration of Brags (Thomas, 1962)

Inelastic interaction is an additional manner incident electron interact with the sample. Incident electrons make inelastic interactions with sample atoms, losing its energy in the process. After then, the electrons travel through the rest of the specimen. “This is how Kikuchi Bands and Electron Energy Loss Spectroscopy (EELS) are generated. The elemental composition and atomic bonding state can be determined using EELS. The targeted region EELS investigation may be quite tiny in TEM because to the high magnification, allowing us to analyse the local chemical composition and further map the elemental composition. Due to Bragg reflection of inelastically dispersed electrons, Kikuchi lines occur in reasonably thick crystals”[34]. They are alternating bright and dark lines in the specimen that are connected to atomic spacing.

4.4.1 TEM Sampling:

Sample preparation is the biggest task because the very thin specimen is required for the TEM analysis, and getting a suitable sample is almost a very long process because it need to produce a sample with a lot of care. Sample preparation required lots of patience as well as time because sometimes it could take from 10 minutes to 1 or 2 days depending upon what kind of properties learn from the material.

Firstly, 100μm sample is cut from the rolled sample by a diamond saw cutter. After that emery paper is to use to further reduce the size of the specimen from 100μm to 40μm. This process will be done as rubbing the sample surface with abrasive paper. To be very careful during the choosing of emery paper size, because abrasive paper can damage the sample up to three times of its grid size, that's why fine emery paper should be used for prevention from the damage of sample. After that multiple 3mm disc will be punched from the 40μm sample by the mechanical punching machine. Figure 4.9 illustration of Mechanical Punching machine and Figure 4.10 shows the process from sample cutting to 3mm punching disk.

Figure 4.9 Mechanical Punching Machine

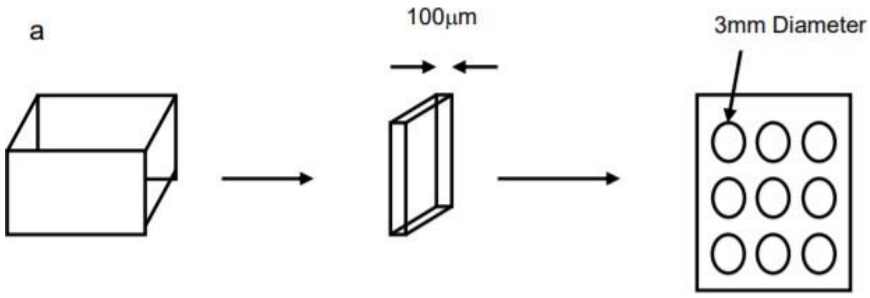

Figure 4.10 Process of cutting sample and punching 3mm disk (David B. Williams, 2009)

After punching 3mm disc from the sample, final mechanical thinning has been done by the ion milling machine. Ion milling is a process for thinned specimens like ceramics and metals in preparation for transmission electron microscopy. A beam of Argon ions impinges on a spinning object in this approach. The Argon gets damaged as a consequence of head-on accidents. Ions will knock away atoms from the specimen, causing the thickness to gradually diminish. The beams are halted as soon as perforation occurs, and final specimen size become 2-3μm and the specimen is delivered to the electron microscope for evaluation. Near the perforation's perimeter, a thin, electron-transparent region is common.

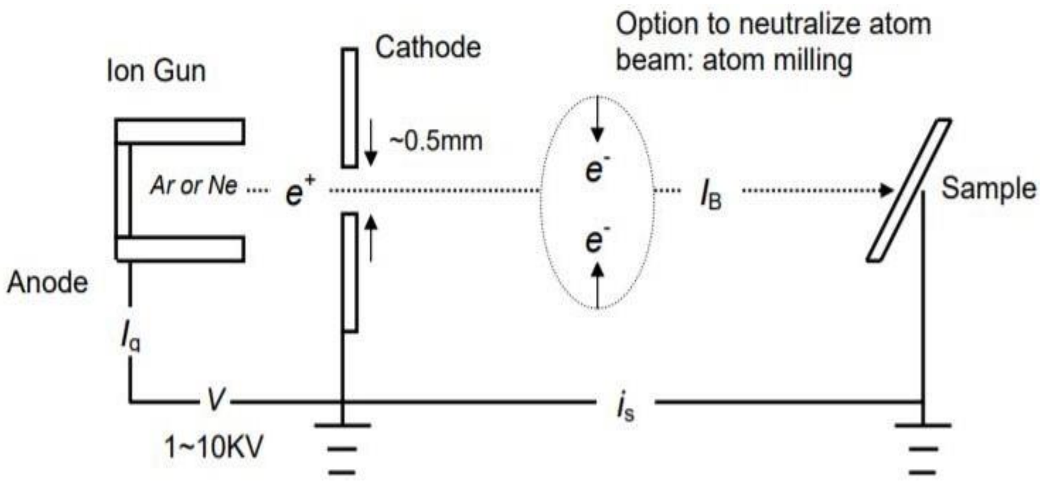

Figure 4.11 illustration of Ion Milling (David B. Williams, 2009)

Chapter.5
Result and Discussion

In the beginning, Mg-0.4wt%Ca cast alloy was synthesized by stir casting process. Stir cast alloy was annealed at 573 K for 24h, followed by quenching. From annealed alloy, circular slices of 10 mm diameter and 0.85 mm thickness were prepared. These circular slices were subjected to high pressure torsion (HPT) processing technique for N = 0, 1/4, 1/2, 1 and 5 revolutions at 300 K , 5 GPa, 1 rpm and a strain rate of $10^{-1}s^{-1}$. In order to compare the microstructure stability, stir cast ingot was also extruded at 473 K, strain rate of $0.25 \times 10^{-3}s^{-1}$.

Figure 5.1a shows the bright field transmission electron microscope(BFTEM) image of completely recrystallized Mg-0.4wt%Ca alloy processed by HPT processing after N = 5 turns. The corresponding selected area diffraction pattern (SAED) acquired shown in Figure 5.1b depicts ring type concentric circles, which confirms the occurrence of recrystallization phenomenon in the sample after 5 revolutions. The average grain size of the alloy was found to be 90 nm.

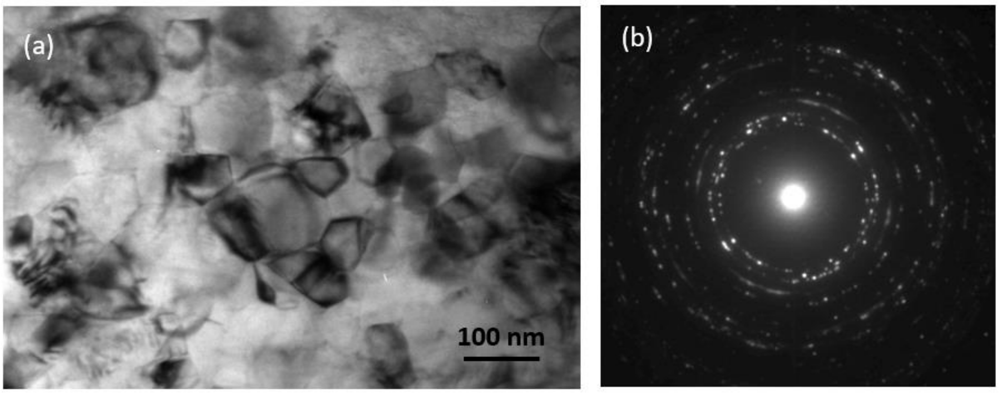

Figure 5.1. (a) BFTEM image of Mg – 0.4Ca alloy processed by HPT(High Pressure Torsion) Technique. After N = 5 turns complete recrystallization occurred. (b) Showing corresponding SAED pattern acquired from several grains.

In order to investigate the segregation phenomena in Mg-0.4Ca HPT N = 5 alloy, scanning transmission electron microscope-high angle annular dark field and low angle annular dark field (STEM-HAADF and LAADF) imaging was carried out(Fig 5.2a&b). Fig 5.2b shows the STEM-LAADF image which was acquired with camera length (CL) = 100 mm to observe the diffraction contrast information from different grains. Fig 5.2a shows the STEM-HAADF image which was acquired with camera length (CL) = 80 mm to observe the Z-contrast information from grain boundaries. However, no Z-contrast was observed from grain boundaries in STEM-HAADF image, which means no segregation of Ca to grain boundaries occurred during HPT at room temperature. Despite the sample was processed at high strain rate, the non-occurrence of Ca segregation shows the requirement of high thermal activation energy.

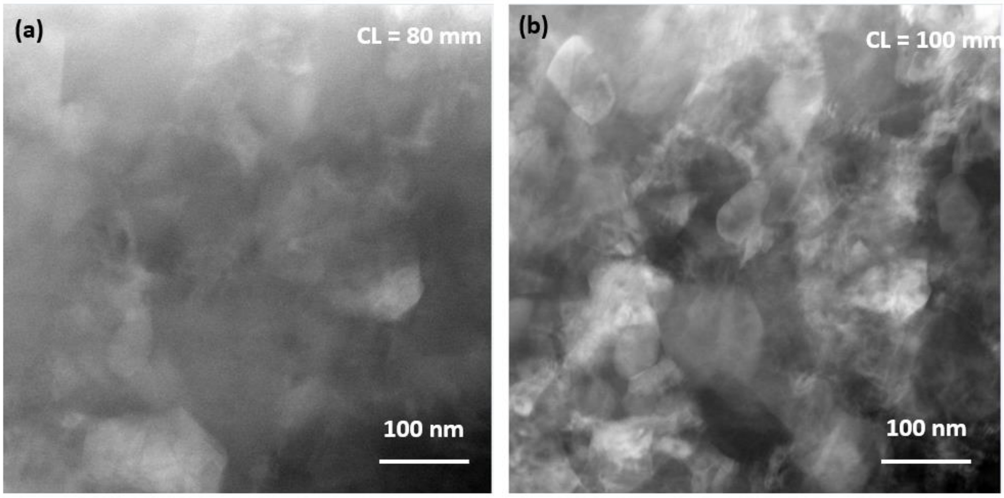

Figure 5.2. (a) STEM-HAADF image did not show any bright contrast from grain boundary which indicates no segregation phenomenon occurred. (b) STEM-LAADF image showing the diffraction contrast from the different grains.

In order further verify the segregation phenomena in Mg-0.4Ca HPT N = 5 alloy, STEM-EDS line profile analysis was carried out across the grain boundary as shown in Fig 5.3a. The line profile did not show peak at the grain boundary which can be evident from the plot as shown in Fig 5.3b. Hence, no Ca segregation was detected through STEM-EDS profile also.

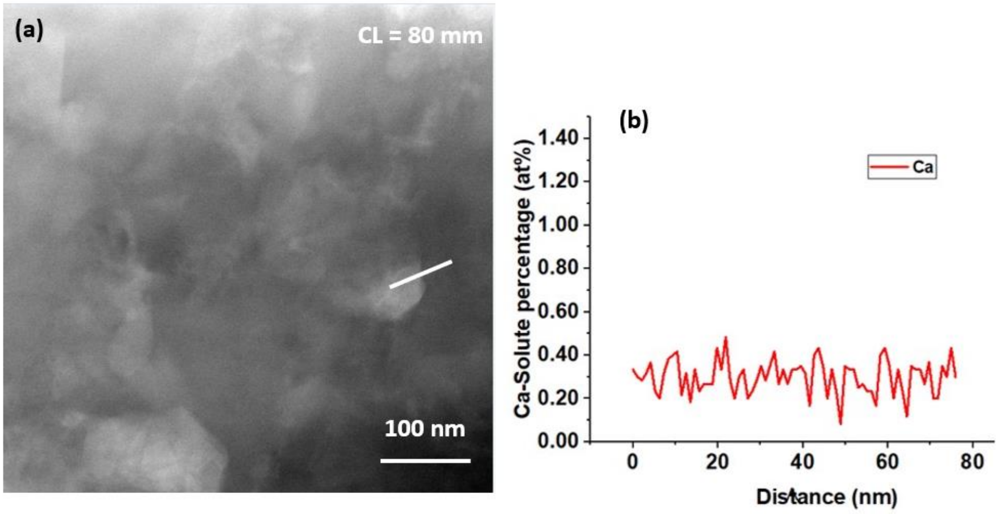

Figure 5.3. (a) STEM-HAADF image showing the grain boundary across which the STEM-EDS line profile was conducted (in Mg-0.4Ca HPT N = 5 alloy). (b) STEM-EDS line profile plot showing no peak from grain boundary which indicates no grain boundary segregation of Ca.

Figure 5.4 shows the bright field transmission electron microscope (BFTEM) image of completely recrystallized Mg-0.4wt%Ca alloy processed by Extrusion technique. The average grain size of the alloy was found to be 4 µm.

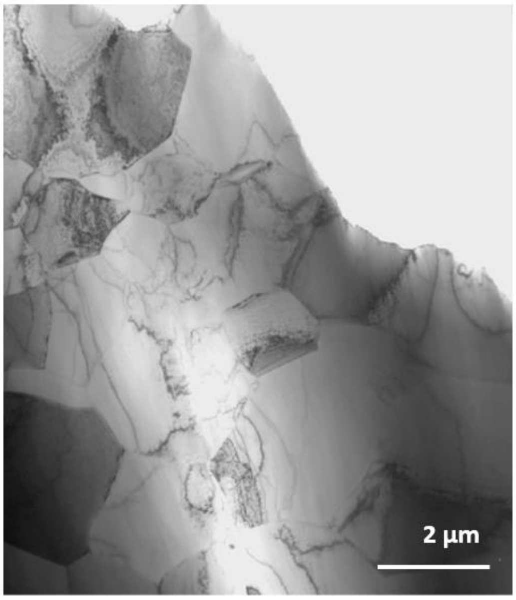

Figure 5.4. BFTEM image showing recrystallized grains in Mg – 0.4Ca alloy processed by Extrusion Technique.

In order to investigate the segregation phenomena in Mg – 0.4Ca alloy processed by extrusion technique, scanning transmission electron microscope-high angle annular dark field and low angle annular dark field (STEM-HAADF and LAADF) imaging was carried out (Fig 5.5a-c). Fig 5.5a shows the STEM-LAADF image which was acquired with camera length (CL) = 200 mm to observe the diffraction contrast information from different grains. Fig 5.5b shows the STEM-LAADF image acquired from another location at high magnification. Fig 5.5c shows the STEM-HAADF image which was acquired with camera length (CL) = 80 mm to observe the Z-contrast information from the boxed region shown in Fig 5.5b. Then the bright-contrast was observed from grain boundaries in STEM-HAADF image, which means segregation of Ca to grain boundaries occurred during extrusion at high temperature.

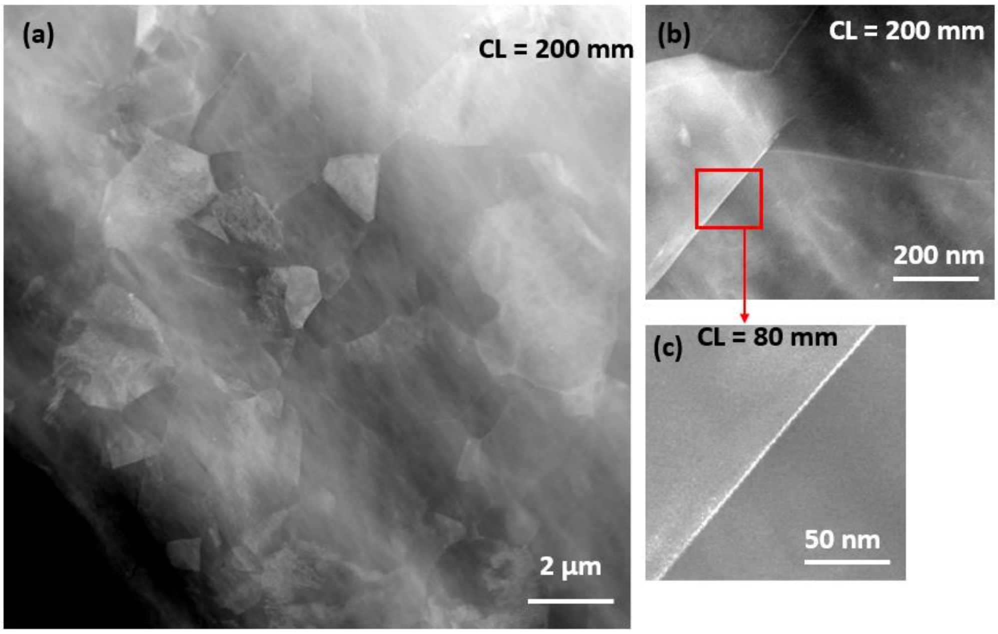

Figure 5.5. (a) STEM-LAADF image acquired with CL = 200 mm showing the diffraction contrast from the different grains in Mg – 0.4Ca extruded alloy. (b) STEM-LAADF image acquired from another location at high magnification. (c) STEM-HAADF image acquired with camera length (CL) = 80 mm from the boxed region in Fig.5b showing Ca segregation to the grain boundaries.

In order further verify the segregation phenomena in Mg – 0.4Ca extruded alloy, STEM-EDS line profile analysis was carried out across the grain boundary as shown in Fig 5.6a. The line profile shows the peak at the grain boundary which can be evident from the plot as shown in Fig 5.6b. Hence, Ca segregation was detected through STEM-EDS profile also.

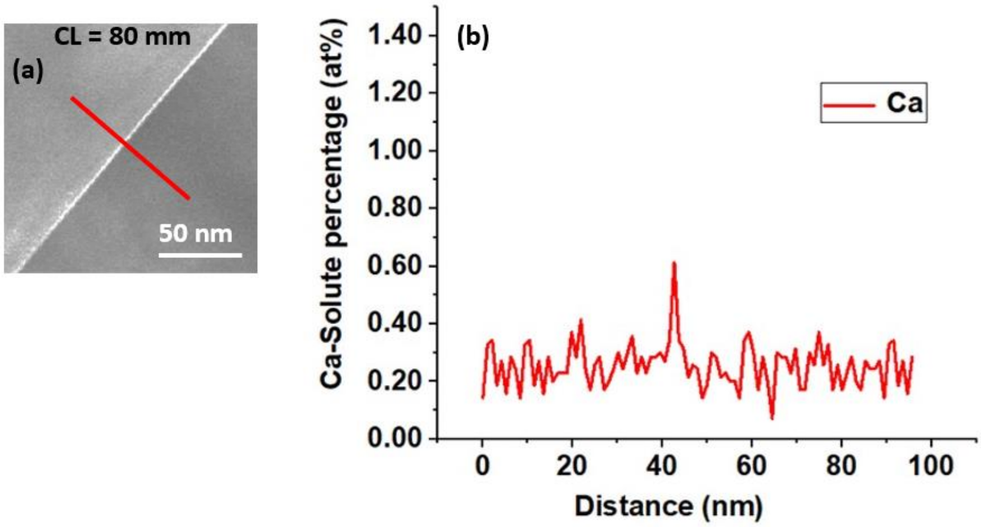

Figure 5.6. (a) STEM-HAADF image showing the grain boundary across which the STEM-EDS line profile was conducted (in Mg – 0.4Ca extruded alloy). (b) STEM-EDS line profile plot showing peak from grain boundary which indicates grain boundary segregation of Ca.

In order to study the microstructure stability of Mg – 0.4Ca HPT and Extrusion processed alloys, the two specimens were heat treated at 573 K for 1 hour. Figure 5.7a shows the bright field transmission electron microscope(BFTEM) image of the heat treated Mg-0.4wt%Ca HPT processed alloy after N = 5 turns. Figure 5.7b shows the STEM-LAADF image of the heat treated Mg-0.4wt%Ca extrusion processed alloy. The average grain size of the HPT and Extrusion processed alloys was found to be 22 µm and 12 µm respectively. From the above observations it can be predicted that the segregation of Ca in extrusion case is more effective in preventing the grain growth of the alloy. The summary of the grain sizes of the alloys processed by HPT and Extrusion methods before and after heat treatment is shown in Fig 5.7c and Table.3

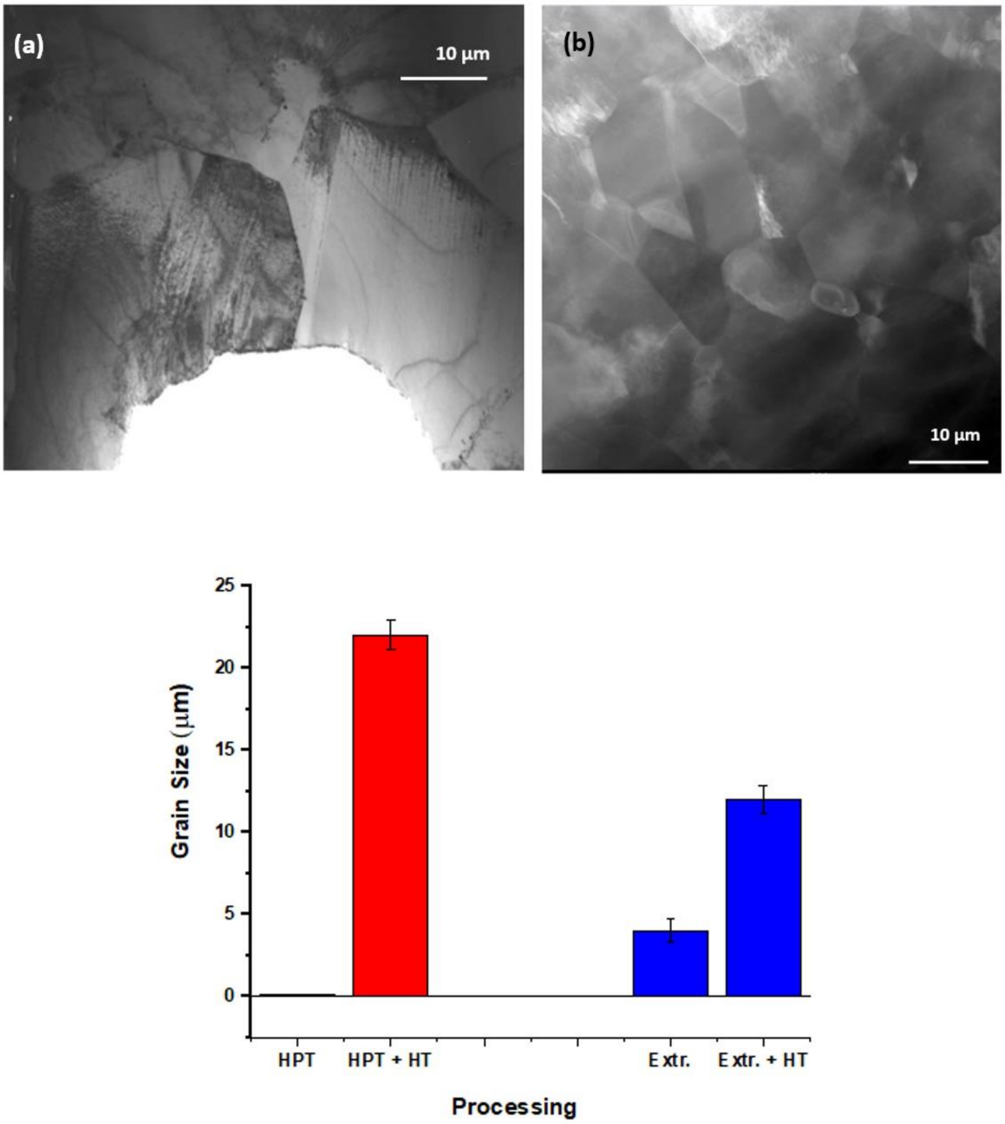

Figure 5.7 (a) BFTEM image of the heat treated Mg-0.4wt%Ca HPT processed alloy after N = 5 turns. (b) STEM-LAADF image of the heat treated Mg-0.4wt%Ca extrusion processed alloy. (c) Plot showing the grain sizes of the alloys processed by HPT and Extrusion methods before and after heat treatment at 573 K for 1 hour.

Table-3: The summary of the grain sizes of the alloys processed by HPT and Extrusion methods before and after heat treatment.

	Average Grain Size (µm)	
	Initial (Before HT)	Final (After HT)
HPT specimen (with out segregation)	0.09	22
Extruded specimen (with	4	12

segregation)		

The hardness measurements of the alloys processed by HPT and Extrusion methods before and after heat treatment are shown in Fig. 8. As the grain size in HPT processed alloy is much lower than the extrusion processed alloy before heat treatment, the hardness of HPT processed alloy is much higher than the extrusion processed alloy. However, after heat treatment, the grain size in HPT processed alloy is increased slightly higher than the extrusion processed alloy, and consequently the hardness of HPT processed alloy is observed to be slightly lower than the extrusion processed alloy.

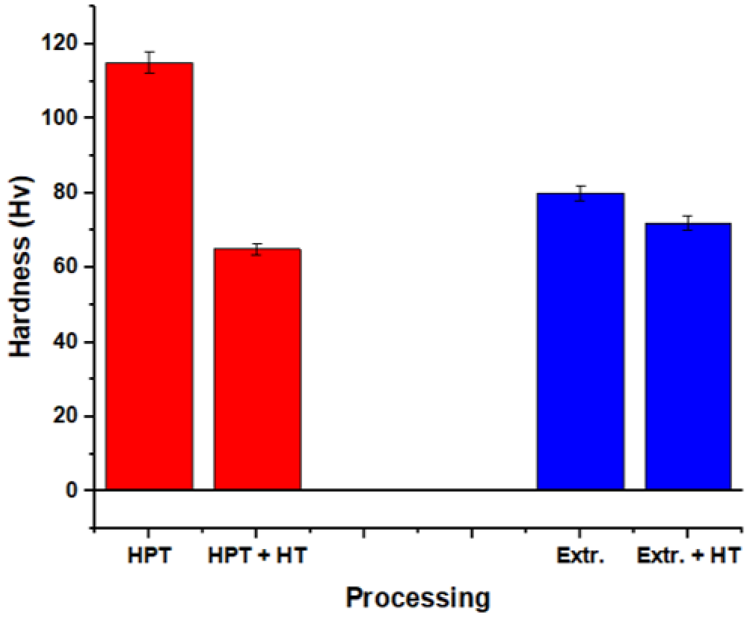

Chapter.6

Conclusions

In the present work, Mg-0.4wt%Ca alloy was processed by HPT at 300 K , 5 GPa, 1 rpm and a strain rate of $10^{-1}s^{-1}$ and Extrusion technique at 473 K, strain rate of $0.25 \times 10^{-3}s^{-1}$.

1. In HPT processed alloy at RT, recrystallization occurred after N = 5 turns. From BFTEM imaging, the average grain size was found to be 90 nm. Based on STEM-HAADF imaging and STEM-EDS analysis it has been found that the segregation of Ca was not observed. It seems higher thermal activation energy required for occurrence of segregation.

2. In extruded alloy at 473 K, from BFTEM imaging, the average grain size was found to be 4 µm. From STEM-HAADF imaging and STEM-EDS analysis it has been found that the segregation of Ca was detected along the grain boundaries.

3. In order to study the microstructure stability of the HPT and Extrusion processed alloys, the two alloys were heat treated at 573 K for 1 hour. The average grain size of the HPT and Extrusion processed alloys was found to be 22 µm and 12 µm respectively. The reason for increase in grain size of HPT alloy was expected to be lack of segregation along grain boundaries.

4. Before heat treatment, the hardness of HPT processed alloy was found to be much higher than the extrusion processed alloy. While, after heat treatment, the hardness of HPT processed alloy is observed to be slightly lower than the extrusion processed alloy. The reasons can be expected from difference in grain sizes of the alloys.

References

[1]. S.M. He, L. P. (2005). Journal of Magnesium and Alloys.

[2]. A.Vinogradov, D. O. (2013). Effect of grain size on the mechanisms of plastic deformation in wrought Mg-Zn-Zr alloy revealed by acoustic emission measurements. Acta Materialia.

[3]. A.H. Musfirah, A. J. (2012). Magnesium and Aluminum Alloys in Automotive Industry. Journal of Applied Sciences Research.

[4]. Agnew S.R, H. J. (2002). Transmission electron microscopy investigation of<c+a> dislocations in Mg and α-solid solution Mg-Li alloys.

[5].Metallurgical and Materials Transactions. al, Y. Z. (2009). Formation of single and multiple deformation twins in nanocrystalline . Acta Materialia.

[6].Amol D. Sable, S. D. (2012). Prepration of Metal Matrix Composites By Stir Casting Method. IJMET.

[7]. A.Bhattacharya, M. N. (2011). Work-hardening behaviour of Mg single crystals Phil.

[8].Burke E.C, H. W. (1952). Metal. Metal.

[9]. C, T. R. (1967). Internal friction and transmission electron microscopy studies of . Acta Material.

[10].Couret A, C. D. (1985). Scripta Material.

[11].David B. Williams, C. B. (2009). Transmission Electron Microscopy. Springer. Frank F.C, N. J. (1953). Stable dislocations in the common crystal lattices. The Philosophical Magazine.

[12]. Groves G.W, K. A. (1963). Independent slip systems in crystals. The Philosophical Magazine: A Journal of Theoretical Experimental and Applied Physics.

[13]. Kaya, M. P. (2013). Fundamentals of Magnesium Alloy Metallurgy. 2013: Woodhead Publishing.

[14].Kelley E.W, H. J. (1968). The relation between polycrystal

deformation and single-crystal deformation. Metallurgical and Materials Transactions.

[15].Kenneth Kanayo Alaneme, E. A. (2017). Enhancing plastic deformability of Mg and its alloys—A review of. Journal of Magnesium and Alloys.

[16]. L. Jiang, D. Z. (2015). The effect of Sn addition on aging behavior and mechanical properties of wrought AZ80 magnesium alloy. alloys and compounds.

[17]. M. Greger, R. K. (2007). Fracture analysis of selected magnesium alloys after different testing methods. Journal of Achievements of Materials and Manufacturing Engineering.

[18]. Minonishi Y, M. S. (1986). Scripta Material.

[19]. Obara T, Y. H. (1973). Nonbasal deformation modes of HCP metals and alloys: Role of dislocation source and mobility. Acta Material.

[20]. Oliver Kraft, P. A. (2010). Plasticity in Confined Dimensions. Annual Review of Materials Research.

[21]. Polmear, I. (2005). Light Alloys. Butterworth-Heinemann.

[22]. Qian Yu, Z.-W. S. (2010). Strong crystal size effect on deformation twinning Nature.

[23]. Robson, Z. Y. (2008). Review on Research and Development of Magnesium Alloys. Acta Metallurgica Sinica.

[24]. S. Morozumi, M. K. (1976). Electron microscope observation in and . Trans.

[25]. Stohr J.F, P. J. (1972). Electron Microscope Study of Pyramidal Slip {112} in Magnesium. The Philosophical Magazine: A Journal of Theoretical Experimental and Applied Physics.

[26]. Thomas, G. (1962). Transmission Electron Microscopy. John Willy and Sons.

[27]. W.J.KimaH.W.LeeaJ.P.ParkbM.G.KimbU.S.Yoon. (2009). Forging of Mg–3Al– 1Zn–1Ca alloy prepared by high-frequency electromagnetic casting. Materials & Design.

[28].Yoo M H, A. S. (2001). Nonbasal deformation modes of HCP metals and alloys: Role of dislocation source and mobility. Metallurgical and Materials Transactions.

[29]. Z. Ding, S. L. (2018). Recent developments in high-strength Mg-RE-based alloys: Focusing on Mg-Gd and Mg-Y systems. Journal of Magnesium and Alloys.

[30]. Paulmurphyplastic.com.

[31]. En.wikipedia.org

[32]. scholarbank.nus.edu.sg

[33]. Sihang You, Yuanding Huang, Karl Ulrich Kainer, Norbert Hort. "Recent research and developments on wrought magnesium alloys", Journal of Magnesium and Alloys, 2017

[34]. docplayer.net